Mem. S.A.It. Vol. 81, 374

**Memorie** della

# Radio emission from supernovae

K.W. Weiler[1], N. Panagia[2,3,4], R.A. Sramek[5], S.D. Van Dyk[6], C.J. Stockdale[7], and C.L. Williams[8]

1 Naval Research Laboratory, Code 7210, Washington, DC 20375-5351, USA
2 Space Telescope Science Institute, 3700 San Martin Drive, Baltimore, MD 21218, USA
3 INAF/Osservatorio Astrofisico di Catania, Via S. Sofia 78, I-95123 Catania, Italy
4 Supernova Ltd., Olde Yard Village #131, Northsound Road, Virgin Gorda, British Virgin Islands
5 National Radio Astronomy Observatory, PO Box 0, Socorro, NM 87801, USA
6 IPAC/Caltech, Mail Code 100-22, Pasadena, CA 91125, USA
7 Marquette University, Physics Dep., P.O. Box 1881, Milwaukee, WI 53214-1881, USA
8 Mass. Inst. of Technology, Kavli Institute for Astr. and Sp. Res., Cambridge, MA 02139

**Abstract.** Study of radio supernovae over the past 30 years includes more than three dozen detected objects and more than 150 upper limits. From this work it is possible to identify classes of radio properties, demonstrate conformance to and deviations from existing models, estimate the density and structure of the circumstellar material and, by inference, the evolution of the presupernova stellar wind, and reveal the last stages of stellar evolution before explosion. Along with reviewing these general properties of the radio emission from supernovae, we present our extensive observations of the radio emission from supernova (SN) 1993J in M 81 (NGC 3031) made with the Very Large Array and other radio telescopes. The SN 1993J radio emission evolves regularly in both time and frequency, and the usual interpretation in terms of shock interaction with a circumstellar medium (CSM) formed by a pre-supernova stellar wind describes the observations rather well considering the complexity of the phenomenon. However: 1) The highest frequency measurements at 85 - 110 GHz at early times (< 40 days) are not well fitted by the parameterization which describes the cm wavelength measurements. 2) At a time ∼ 3100 days after shock breakout, the decline rate of the radio emission steepens from ($t^{+\beta}$) $\beta \sim -0.7$ to $\beta \sim -2.7$ without change in the spectral index ($\nu^{+\alpha}$; $\alpha \sim -0.81$). This decline is best described not as a power-law, but as an exponential decay with an e-folding time of ∼ 1100 days. 3) The best overall fit to all of the data is a model including both non-thermal synchrotron self-absorption (SSA) and a thermal free-free absorbing (FFA) components at early times, evolving to a constant spectral index, optically thin decline rate, until a break in that decline rate at day ∼ 3100, as mentioned above.

**Key words.** radio continuum:stars − supernovae

## 1. Introduction

A series of papers on radio supernovae (RSNe) has established the radio detection and, in a

*Send offprint requests to*: K. Weiler

number of cases, radio evolution for more than three dozen supernovae (SNe). A much larger list of more than 150 additional SNe have low radio upper limits (See *http://rsd-www.nrl.navy.mil/7213/weiler/kwdata/rsnhead.html*). In this extensive study of the radio emission from SNe, several effects have been noted:

- type Ia SNe are not radio emitters to the detection limit of the VLA[1]
- type Ib/c SNe are radio luminous with steep spectral indices (generally $\alpha < -1$; $S \propto \nu^{+\alpha}$) and have a fast turn-on/turn-off, usually peaking at 6 cm near or before optical maximum.
- type II SNe show a range of radio luminosities with flatter spectral indices (generally $\alpha > -1$) and a relatively slow turn-on/turn-off, usually peaking at 6 cm significantly after optical maximum.

Measurements of the multi-frequency radio light curves and their evolution with time show the density and structure of the CSM, evidence for possible binary companions, clumpiness or filamentation in the presupernova wind, mass-loss rates and changes therein for the presupernova stellar system and, through stellar evolution models, estimates of the ZAMS presupernova stellar mass and the stages through which the star passed on its way to explosion.

Of particular recent interest are the radio observations of SN 1993J in M 81 (NGC 3031) which was discovered at magnitude $V \sim 11.8$ mag on 28.91 March 1993 (Ripero, Garcia, & Rodriguez 1993), and by 30 March, at maximum optical magnitude $V = 10.7$ mag, had become the brightest supernova in the northern hemisphere since SN 1954A. Hydrogen was soon identified in its optical spectrum, classifying it as a type II SN (SNII) (see, e.g., Andrillat et al. 1993; Filippenko et al. 1993).

From the outset, SN 1993J displayed unusual characteristics for a SNII. The visual light curve was markedly different from both the SNIIL (linear) and SNIIP (plateau) subtypes in that it exhibited a second maximum $\sim 17$ days after the first one. Its unusual light curve and spectrum were quickly interpreted by Nomoto et al. (1993) and Swartz et al. (1993) as implying a red supergiant progenitor with a thin hydrogen envelope which would spectrally evolve from resembling a SNII to resembling a SNIb, thereby suggesting a SNIIb classification. Continuing observations of visual spectra by Filippenko, Matheson, & Ho (1993) confirmed this transition.

Radio emission from SN 1993J was detected with the VLA on UT 02.30 April 1993, with a flux density of $0.8 \pm 0.2$ mJy at 1.3 cm (Weiler et al. 1993), [see also (Van Dyk et al. 1993a,b)] and with the Ryle Telescope in Cambridge, UK on UT 5.7 April 1993 at 2 cm Pooley & Green (1993a). By UT 25 April 1993 the rapidly expanding SN already had a measurable size of $0.25 \pm 0.1$ milliarcseconds (mas) with Very Long Baseline Interferometry (VLBI) techniques Marcaide et al. (1993a,b).

High angular resolution VLBI size measurements of the expanding SN were conducted very early by Marcaide et al. (1994) and Bartel et al. (1994) and VLBI monitoring continues to the present at multiple wavelengths [see, e.g., (Bartel et al. 2002; Bietenholtz, Bartel, & Rupen 2001, 2003; Marcaide et al. 1997, 2009)].

Extensive radio monitoring of the integrated flux density of SN 1993J has been conducted by the VLA (Van Dyk et al. 1994; Weiler et al. 2007) and with the Ryle Telescope Pooley & Green (1993b). Very short wavelength observations were conducted with the French-German Institut de Radioastronomie Millimetrique (IRAM) telescope Radford et al. (1993) and at the Caltech Owens Valley Radio Observatory (OVRO) Phillips & Kulkarni (1993a,b). More recently, Chandra, Bhatnagar, & Ray (2001) have conducted longer wavelength observations with the Giant Metrewave Radio Telescope (GMRT) in India.

[1] The VLA telescope of the National Radio Astronomy Observatory is operated by Associated Universities, Inc. under a cooperative agreement with the National Science Foundation.

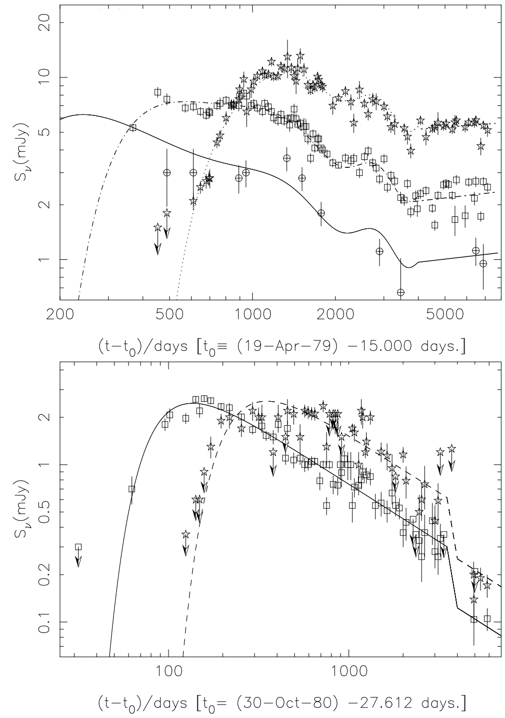


**Fig. 1.** Top: Type II SN 1979C at 2 cm (14.9 GHz; *crossed circles, solid line*), 6 cm (4.9 GHz; *open squares, dash-dot line*), and 20 cm (1.5 GHz; *open stars, dotted line*) [Note that the radio flux density increases after day ∼ 4000 and has a sinusoidal modulation before day ∼ 4000; (Montes et al. 2000; Weiler et al. 1991, 1992).] Bottom: Type II SN 1980K at 6 cm (4.9 GHz; *open squares, solid line*), and 20 cm (1.5 GHz; *open stars, dashed line*). (Note a sharp drop in flux density after day ∼ 4000; (Montes et al. 1998; Weiler et al. 1992)).

## 2. Emission models

All known RSNe appear to share common properties of:

- Nonthermal synchrotron emission with high brightness temperature.
- A decrease in absorption with time, resulting in a smooth, rapid turn-on first at shorter wavelengths and later at longer wavelengths.
- A power-law decline of the flux density with time at each wavelength after maximum flux density (optical depth ∼ 1) is reached at that wavelength.

The characteristic RSN radio light curves arise from the competing effects of slowly declining non-thermal radio emission and more rapidly declining thermal and/or non-thermal absorption yielding a rapid turn-on and slower turn-off of the radio emission at any single frequency. This characteristic light curve shape is illustrated in Figure 1 for SN 1979C and SN 1980K. Since absorption processes are greater at lower frequencies, transition from optically thick to optically thin (turn-on) occurs first at higher frequencies and later at lower frequencies.

Chevalier (1982a,b) has proposed that the relativistic electrons and enhanced magnetic field necessary for synchrotron emission arise from the SN blastwave interacting with a relatively high density CSM which has been ionized and heated by the initial UV/X-ray flash. This CSM density ($\rho$), which decreases as an inverse power, s, of the radius, r, from the star, is presumed to have been established by a presupernova stellar wind with mass-loss rate, $\dot{M}$, and velocity, $w_{\rm wind}$, (i.e., $\rho \propto \frac{\dot{M}}{w_{\rm wind}\ r^s}$) from a massive stellar progenitor or companion. For a constant mass-loss rate and constant wind velocity $s = 2$. This ionized CSM is the source of some or all of the initial thermal gas free-free absorption (FFA). Additionally, Chevalier (1998) has proposed that synchrotron self-absorption (SSA) may play a role in some objects.

A rapid rise in the observed radio flux density results from a decrease in these absorption processes as the radio emitting region expands and the absorption processes, either internal or along the line-of-sight, decrease. Weiler et al. (1990) have suggested that this CSM can be "clumpy" or "filamentary," leading to a slower radio turn-on, and Montes, Weiler, & Panagia (1997) have proposed the possible presence of a distant ionized medium along the line-of-sight which is sufficiently distant from the explosion that it is unaffected by the blastwave and can cause a spectral turn-over at low radio frequencies. In addition to clumps or filaments, the CSM may be radially structured

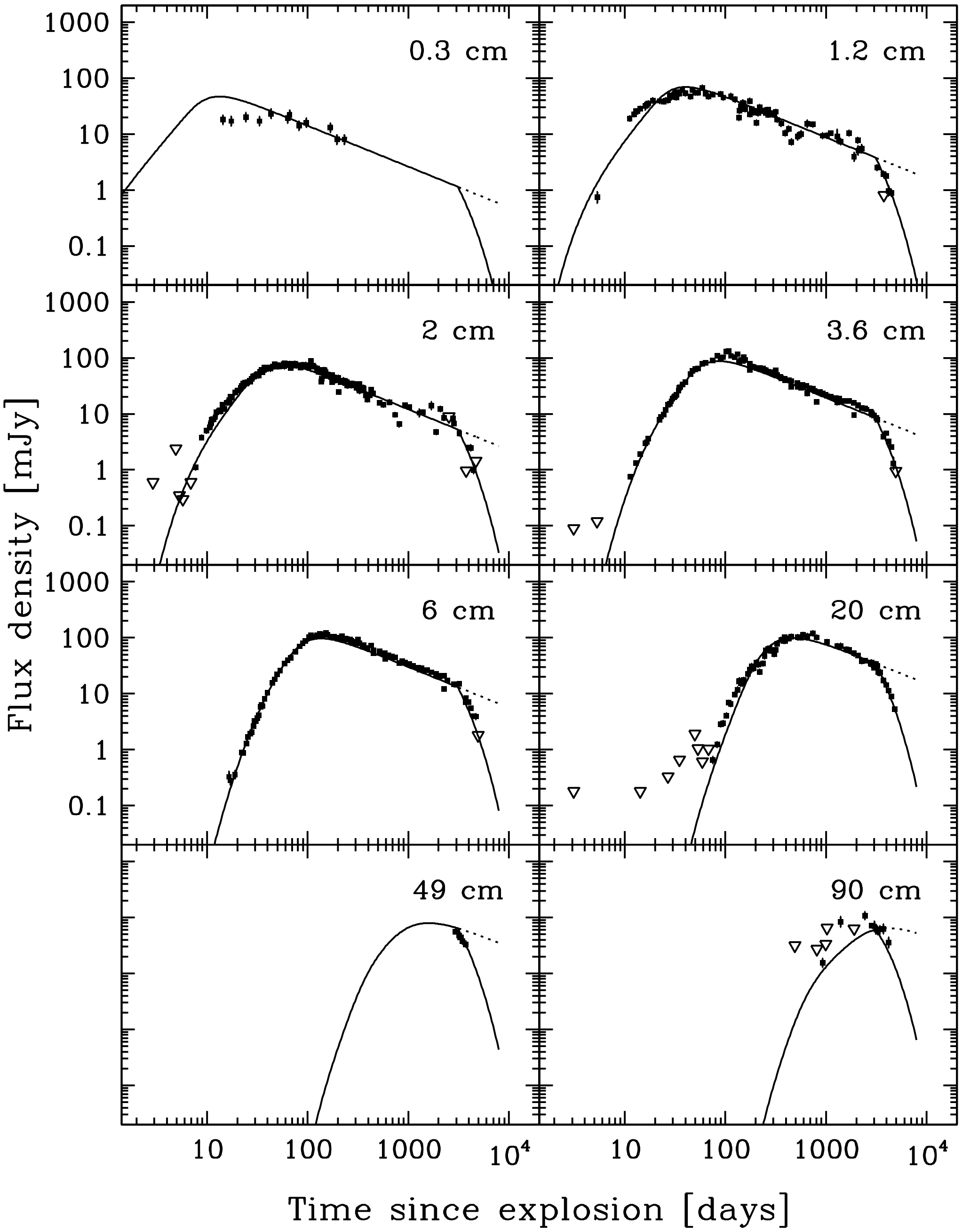


**Fig. 2.** The radio light curves for SN 1993J are plotted from left to right and top to bottom at 0.3, 1.2, 2, 3.6, 6, 20, 49, and 90 cm. The lines represent the best fit combined synchrotron self-absorption (SSA) and thermal, free-free absorption (FFA) model as described in the text and by Weiler et al. (2007) with an exponential flux density decline after day 3100 with an e-folding time of 1100 days. Upper limits ($3\sigma$) are shown as open inverted triangles).

with significant density irregularities such as rings, disks, shells, or gradients.

## 3. Results

The success of the basic parameterization and modeling has been shown in the good correspondence between the model fits and the data for all subtypes of RSNe: e.g., type Ib SN 1983N (Sramek, Panagia, & Weiler 1984), type Ic SN 1990B (Van Dyk et al. 1993a), and type II SN 1979C (Montes et al. 2000; Weiler et al. 1991, 1992) and SN 1980K (Montes et al. 1998; Weiler et al. 1992). (Note that after day $\sim$ 4000, the evolution of the radio emission from both SN 1979C and SN 1980K deviates from the expected model evolution and that SN 1979C shows a sinusoidal modulation in its flux density prior to day ~4000.)

Additionally, in their study of the radio emission from SN 1986J, Weiler et al. (1990) found that the simple Chevalier model could not describe the relatively slow turn-on. They therefore included additional terms in their model [see, e.g., (Weiler et al. 2002, 2003)] which they interpreted (Weiler et al. 1990) to represent the presence of filaments or clumps in the CSM. Such a clumpiness in the wind material was again required for modeling the radio data from SN 1988Z (Van Dyk et al. 1993b; Williams et al. 2002) and SN 1993J Van Dyk et al. (1994). Since that time, evidence for filamentation in the envelopes of SNe has also been found from optical and UV observations (Filippenko, Matheson, & Barth 1994; Spyromilio 1994).

Although there is insufficient space here for detailed discussion, (Weiler et al. 2002, 2003) present equations and examples for estimating mass-loss rates, and changes therein, from presupernova systems, evidence for binarity in presupernova systems, and evidence for ionized hydrogen along the line-of-sight, possibly from the HII region which was the birthplace of the massive supernova progenitor.

## 4. SN1993J

A particularly well studied case of a radio supernova is SN 1993J Weiler et al. (2007) where fitting of the data (see Figure 2) with standard models required splitting it into two parts: an "early" data set from day 0 through day $\sim$ 3100 and a "late" data set for days $\sim$ 3100 through the final measurements on day 4930. The reason for this splitting of the data set was that the decline rate $\beta$ is clearly steepening after day $\sim$ 3100 and appears best described by an exponential with e-folding time of 1100 days rather than the power law decline used at earlier epochs.

The early (day < 3100) data were first fitted with two possible "pure" absorption models, namely pure SSA (i.e. negligible FFA at all times) and pure FFA (i.e. negligible SSA at all times). Weiler et al. (2007) found that both "pure" models were able to represent the light curves as well as the spectral index evolution only roughly. However, for the pure SSA model the rising branch of the light curve at early times was "too straight" in that it could not reproduce the apparent curvature in the flux density turn-on that is most noticeable at frequencies lower than 5 GHz. Also, the spectral index evolution at early times for pure SSA was inadequate to represent the observations. Moreover, the corresponding brightness temperature evolution was rather strange in that the temperature appeared to peak at later times for lower frequencies.

For the pure FFA model the rising branch of the light curves appeared to provide a better fit for both the light curves and the spectral index, but it failed the test of the brightness temperature. After correction for the external, thermal absorption, the implied brightness temperature at early times, for several frequencies, exceeded the physical limit of $T_B \simeq 3 \times 10^{11}$ K (see, e.g., Readhead 1994).

The best results were achieved with a model that comprised both SSA and FFA and the results are displayed in Figures 2, 3, and 4 which show the light curves, the spectral index evolution, and the brightness temperature evolution, respectively. As mentioned above, after day $\sim$ 3100 an exponential with an e-folding

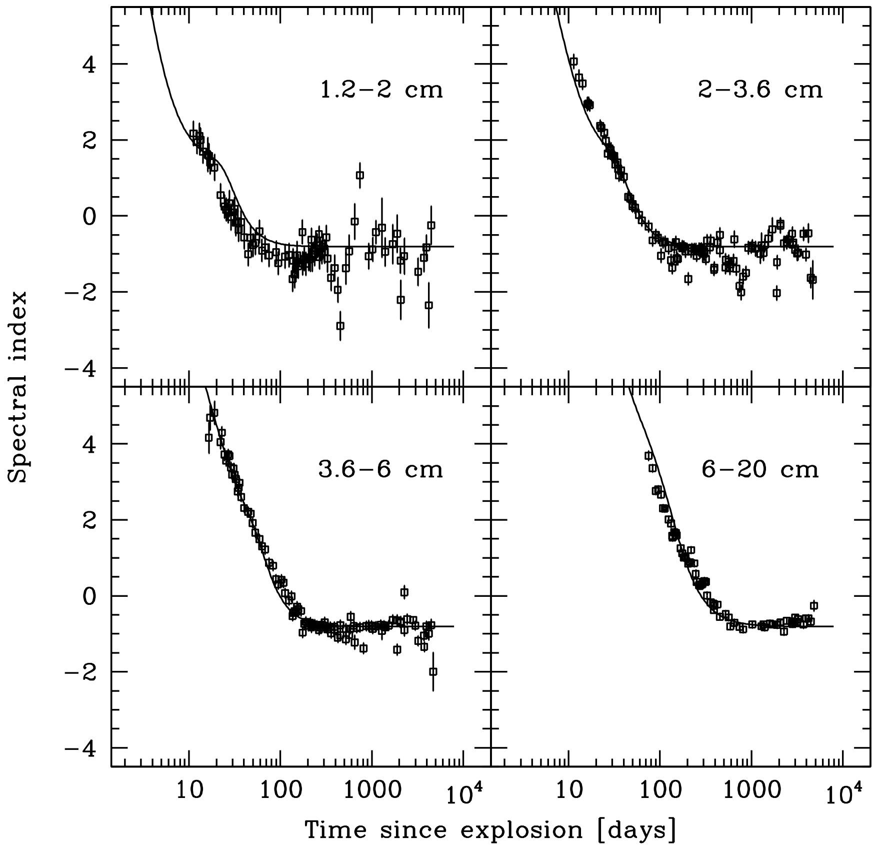


**Fig. 3.** The spectral index ($\alpha$; S $\propto \nu^{+\alpha}$) evolution for SN 1993J between 1.2 and 2 cm (top left), between 2 and 3.6 cm (top right), between 3.6 and 6 cm (bottom left), and between 6 and 20 cm (bottom right). As in Figure 2 the lines represent the best fit combined synchrotron self-absorption (SSA) and thermal, free-free absorption (FFA) model as described in the text and by Weiler et al. (2007).

time of 1100 days is the plotted curve to show the sharp drop-off in flux density.

## 5. Conclusions

The success of the basic parameterization and modeling is shown in the good agreement between the model fits and the data for all subtypes of RSNe. Thus, the radio emission from SNe appears to be relatively well understood in terms of blastwave interaction with a structured CSM and allows description of such progenitor system properties as mass-loss rate, change in mass-loss rate, filamentation or clumpiness, binarity, and remote HII, as well as estimates of progenitor properties.

We also discuss detailed radio observations of SN 1993J at multiple wavelengths for ~ 13 years after explosion. The radio emission for SN 1993J evolves regularly in both time and frequency, and the usual interpretation in terms of shock interaction with a complex circumstellar medium (CSM) formed by a pre-supernova stellar wind, and the inclusion of thermal and/or non-thermal absorption at early times, describes the observations rather well considering the complexity of the phenomenon. However, there are some notable characteristics peculiar to SN 1993J. 1) At a time around day ~ 3100 after shock breakout the decline rate of the radio emission steepens from ($t^{+\beta}$) $\beta$ ~ −0.7 to $\beta$ ~ −2.7 with-

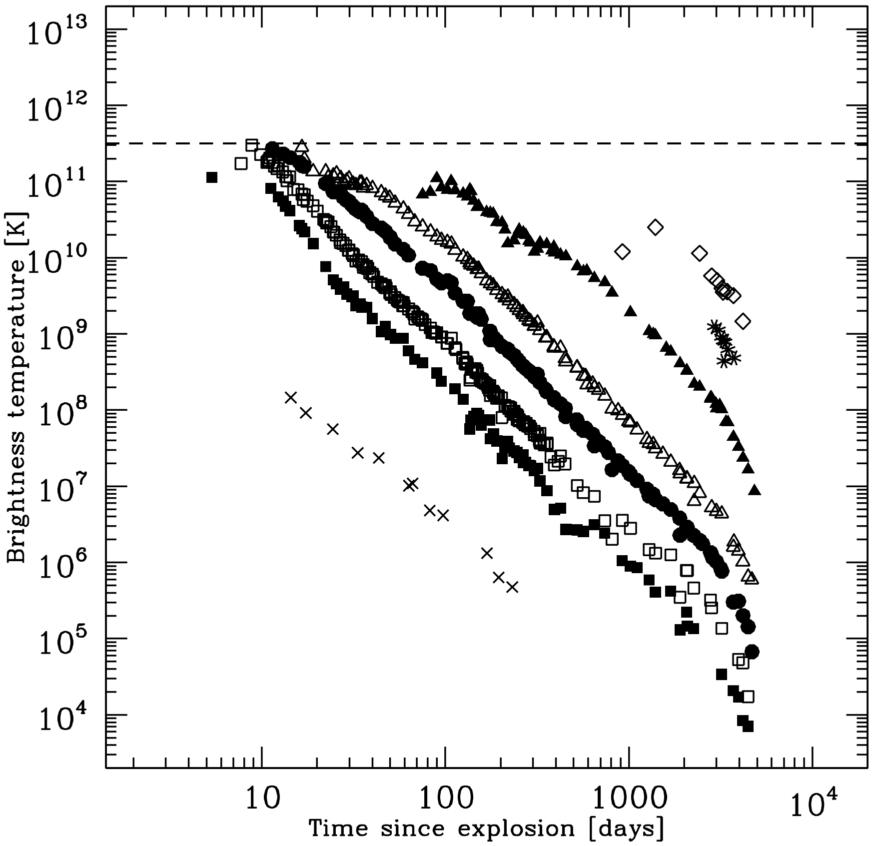


**Fig. 4.** The brightness temperature ($T_B$) evolution for SN 1993J for, from left to right, 0.3 (×), 1.2 (filled squares), 2 (open squares), 3.6 (filled circles), 6 (open triangles), 20 (filled triangles), 49 (∗), and 90 (open diamonds) cm corrected for extended, free-free absorption flux density suppression at early times as described in the text and by Weiler et al. (2007). The horizontal dashed line denotes the limiting value of $T_B \simeq 3 \times 10^{11}$ K Readhead (1994), which is not exceeded at any frequency.

out change in the spectral index ($\nu^{+\alpha}$; $\alpha \sim -0.81$). This variation, however, can better be described in terms of an exponential decay starting at day ∼ 3100 with an e-folding time of ∼ 1100 days. 2) The spectral index appears constant throughout our measurement era. 3) The best overall fit to all of the "early" (i.e., before day 3100) data is a model including both non-thermal synchrotron self-absorption (SSA) and thermal free-free absorbing (FFA) components, evolving to a constant decline rate until the break at day ∼ 3100. In particular, neither a pure SSA nor a pure FFA absorbing model can provide a fit that simultaneously reproduces the light curves and the spectral index evolution and provides a physically realistic brightness temperature evolution.

*Acknowledgements.* KWW wishes to thank the Office of Naval Research (ONR) for the 6.1 funding supporting his research. CJS is a Cottrell Scholar of Research Corporation and work on this project has been supported by the NASA Wisconsin Space Grant Consortium. NP is Astronomer Emeritus at the Space Telescope Science Institute (STScI) that kindly provided research facilities and partial support for this work.

## References


Andrillat, Y., Prugniel, P., Perelmuter, J.-M., Shanklin, J. D., Kohl, R., Cianciolo, F., Gearhart, R., & Dosaj, A. 1993, IAU Circ., 5736

Bartel, N. et al. 1994, Nature, 368, 610

Bartel, N. et al. 2002, ApJ, 581, 404

Bietenholz, M. F., Bartel, N., & Rupen, M. P. 2001, ApJ, 557, 770

Bietenholz, M. F., Bartel, N., & Rupen, M. P. 2003, ApJ, 597, 374

Chandra, P., Bhatnagar, S., & Ray, A. 2001, IAU Circ., 7657

Chevalier, R. A., 1982a, ApJ, 259, 302

Chevalier, R. A. 1982b, ApJ, 259, L85

Chevalier, R. A. 1998, ApJ, 499, 810

Filippenko, A. V., Matheson, T., Kirshner, R. P., Schmidt, B. P., Caldwell, N., Merlin, J.-C., Neely, A., Schmeer, P., & Vanmunster, T., 1993, IAU Circ., 5740

Filippenko, A. V., Matheson, T., & Ho., L., 1993, ApJ, 415, L103

Filippenko, A., Matheson, T., & Barth, A., 1994, AJ, 108, 222

Marcaide, J. M. et al. 1993a, IAU Circ., 5785

Marcaide, J. M. et al. 1993b, IAU Circ., 5820

Marcaide, J. M. et al. 1994, ApJ, 424, L25

Marcaide, J. M. et al. 1997, ApJ, 486, L31

Marcaide, J. M. et al. 2009, A&A, submitted

Montes, M. J., Weiler, K. W., & Panagia, N., 1997, ApJ, 488, 792

Montes, M. J., Van Dyk, S. D., Weiler, K. W., Sramek, R. A., & Panagia, N., 1998, ApJ, 506, 874

Montes, M. J., Weiler, K. W., Van Dyk, S. D., Panagia, N., Lacey, C. K., Sramek, R. A., & Park, R., 2000, ApJ, 532, 1124

Nomoto, K., Suzuki, T., Shigeyama, T., Kumagai, S., Yamaoka, H., & Saio, H., 1993, Nature, 364, 507

Phillips, J. A. & Kulkarni, S. R., 1993a, IAU Circ., 5763

Phillips, J. A. & Kulkarni, S. R., 1993b, IAU Circ., 5775

Pooley, G. G. & Green, D. A., 1993a, IAU Circ., 5751

Pooley, G. G. & Green, D. A., 1993b, MNRAS, 264, 17P

Radford, S., Neri, R., Guilloteau, S., & Downes, D., 1993, IAU Circ., 5768

Readhead, A. C. S., 1994, ApJ, 426, 51

Ripero, J., Garcia, F., & Rodriguez, D., 1993, IAU Circ., 5731

Spyromilio, J., 1994, MNRAS, 266, 61

Swartz, D. A., Clocchiatti, A., Benjamin, R., Lester, D. F., & Wheeler, J. C., 1993, Nature, 365, 232

Sramek, R. A., Panagia, N., & Weiler, K. W., 1984, ApJ, 285, L59

Van Dyk, S. D., Weiler, K. W., Rupen, M. P., Sramek, R. A., & Panagia, N., 1993a, IAU Circ., 5759

Van Dyk, S. D., Nguyen, H.-A., Weiler, K. W., Sramek, R. A., Rupen, M. P., & Panagia, N., 1993b, IAU Circ., 5828

Van Dyk, S. D., Weiler, K. W., Sramek, R. A., Rupen, M. P., & Panagia, N., 1994, ApJ, 432, L115

Weiler, K. W., Panagia, N., & Sramek, R. A., 1990, ApJ, 364, 611

Weiler, K. W., Van Dyk, S. D., Panagia, N., Sramek, R. A., & Discenna, J., 1991, ApJ, 380, 161

Weiler, K. W., Van Dyk, S. D., Pringle, J., & Panagia, N., 1992, ApJ, 399, 672

Weiler, K. W., Van Dyk, S. D., Panagia, N., & Sramek, R. A., 1992, ApJ, 398, 248

Weiler, K. W., Sramek, R. A., Van Dyk, S. D., & Panagia, N., 1993, IAU Circ., 5752

Weiler, K. W., Panagia, N., Montes, M. J., & Sramek, R. A., 2002, ARA&A, 40, 387

Weiler, K. W., Panagia, N., & Montes, M. J., in "Supernovae and Gamma-Ray Bursters," K. W. Weiler, ed., 2003, Springer-Verlag, Berlin, p. 367

Weiler, K. W., Williams, C. L., Panagia, N., Stockdale, C. J., Kelley, M. T., Sramek, R. A., Van Dyk, S. D., & Marcaide, J. M., 2007, ApJ, 671, 1959

Williams, C. L., Panagia, N., Lacey, C. K., Weiler, K. W., Sramek, R. A., & Van Dyk, S. D., 2002, ApJ, 581, 396